Special Section: Patterns

H.R. Bogena*
M. Herbst
J.A. Huisman
U. Rosenbaum
A. Weuthen
H. Vereecken

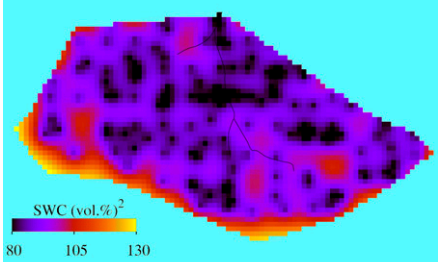

Wireless sensor networks are an exciting new technology for near-real-time monitoring of soil water content (SWC). In this study, we developed the SoilNet technology and analysed six million SWC measurements from a 4-mo period to explore SWC variability at the headwater catchment scale.

Agrosphere Inst., ICG-4, Forschungszentrum Jülich GmbH, 52425 Jülich, Germany. *Corresponding author (h.bogena@fz-juelich.de).

Vadose Zone J. 9:1002–1013
doi:10.2136/vzj2009.0173
Received 30 Nov. 2009.
Published online 7 Sept. 2010.

Potential of Wireless Sensor Networks for Measuring Soil Water Content Variability

Soil water content (SWC) plays a key role in partitioning water and energy fluxes at the land surface and in controlling hydrologic fluxes such as groundwater recharge. Despite the importance of SWC, it is not yet measured in an operational way at larger scales. The aim of this study was to investigate the potential of wireless sensor network technology for the near-real-time monitoring of SWC at the field and headwater catchment scales using the recently developed wireless sensor network SoilNet. The forest catchment Wüstebach (~27 ha) was instrumented with 150 end devices and 600 EC-5 SWC sensors from the ECH_2O series by Decagon Devices. In the period between August and November 2009, more than six million SWC measurements were obtained. The observed spatial variability corresponded well with results from previous studies. The very low scattering in the plots of mean SWC against SWC variance indicates that the sensor network data provide a more accurate estimate of SWC variance than discontinuous data from measurement campaigns, due, e.g., to fixed sampling locations and permanently installed sensors. The spatial variability in SWC at the 50-cm depth was significantly lower than at 5 cm, indicating that the longer travel time to this depth reduced the spatial variability of SWC. Topographic features showed the strongest correlation with SWC during dry periods, indicating that the control of topography on the SWC pattern depended on the soil water status. Interpolation results indicated that the high sampling density allowed capture of the key patterns of SWC variation.

Abbreviations: AIC, Akaike information criterion; SWC, soil water content; WI wetness index.

A remaining challenge in hydrology is to explain the observed patterns of hydrologic behavior across multiple space–time scales as a result of interacting environmental factors. The large spatial and temporal variability of soil water content (SWC) is determined by factors like atmospheric forcing, topography, soil properties, and vegetation, which interact in a complex, nonlinear way (e.g., Grayson et al., 1997; Western et al., 2004). Understanding and characterizing this spatial variability is one of the major challenges within hydrologic science (Vereecken et al., 2007). Nevertheless, in a system of potentially unlimited complexity and heterogeneity, the amount and quality of data clearly limits the amount of extractable knowledge (Thierfelder et al., 2003).

To determine the spatiotemporal structure of hydrologic state variables, an enormous measurement effort is necessary. In the case of SWC, remote sensing technologies, such as passive or active microwave radiometry, can avoid direct measurements by providing area-wide estimates of surface SWC (e.g., Wigneron et al., 2003; Löw et al., 2006); however, the received signal is strongly influenced by vegetation and surface roughness, and the sampling depth is restricted to the uppermost soil (2–5 cm) (Walker et al., 2004). Consequently, direct measurements are still indispensable in areas with significant vegetation and litter cover. Typically, the footprint scale ranges from about 100 m for an airborne radiometer (e.g., a polarimetric L-band multibeam radiometer), to about 50 km for a space-borne radiometer (e.g., the Soil Moisture and Ocean Salinity satellite). Given the high variability of SWC, a large number of ground measurements are needed to estimate the mean SWC within a remotely sensed footprint for validation purposes (Ryu and Famiglietti, 2005).

Catchment-wide information about SWC dynamics at multiple depths is also highly desirable to quantify hydrologic fluxes as well as fluxes at soil–vegetation–atmosphere interfaces (Robinson et al., 2008). These fluxes are nonlinearly related to SWC and, therefore, ignoring its subgrid-scale heterogeneity often produces significant bias in large-scale simulations of water and energy fluxes (e.g., Crow and Wood, 2002). To reduce this error, subgrid SWC variability is often parameterized using the SWC variance. Unfortunately, there are

only very few data sets with measurements of both catchment-wide SWC dynamics in the topsoil and measurements of the SWC of the subsoil (Vereecken et al., 2008). These examples illustrate that there is still a need for measurement techniques that can assess large-scale, three-dimensional SWC fields with high temporal and spatial resolution (Schulz et al., 2006).

A promising new technology for monitoring SWC dynamics at multiple depths is the wireless sensor network (Cardell-Oliver et al., 2005; Ritsema et al., 2009; Trubilowicz et al., 2009). The aim of this study was to: (i) present the novel wireless sensor network SoilNet developed at the Forschungszentrum Jülich; and (ii) illustrate the potential of wireless sensor networks for the analysis of SWC patterns and hydrologic processes at the catchment scale.

Wireless Sensor Network Technology

Although wireless sensor networks can still be considered as an emerging research field, the supporting communication technology for low-cost, low-power, wireless networks has matured greatly in the past decade (Robinson et al., 2008). Wireless environmental sensor networks enable the observation of SWC variability in space and time in near real time. They will play an important role in the emerging terrestrial environmental observatories (Bogena et al., 2006) because they are able to bridge the gap between local- (e.g., lysimeter) and regional-scale measurements (e.g., remote sensing).

One widespread wireless communication technology is called the ZigBee Alliance, which is a low-cost mesh networking proprietary standard (ZigBee Alliance, 2010). The low cost allows the technology to be widely deployed in wireless control and monitoring applications. ZigBee is a suite of high-level communication protocols that uses small, low-power digital radios based on the IEEE 802.15.4 standard for wireless personal area networks (e.g., Kuorilehto et al., 2007). One of the first applications of the ZigBee technology for monitoring soil properties was presented by Valente et al. (2006). Recently, alternative communication technologies have been developed, such as ZigBeePro (e.g., Digi International, 2010) and JenNet (Jennic Ltd., 2009a,b).

The basic structure of a wireless network is presented in Fig. 1. Typically, three different components are present in a wireless network application. The *coordinator* is the top of the network tree. It stores information about the network and it can provide a link to other networks. Each network has only a single coordinator. An important task of the coordinator is to initiate the wireless links within the network. The second component is the *router*, which acts as a relay station that passes data from other devices. The third component is the *sensor*, which should have just enough functionality to communicate with its parent node (either the coordinator or a router). This allows the sensor to be asleep a significant amount of the time to save energy.

Each component of the network has a radio module that consists of several layers. The software interfaces link the hardware components (physical layer and peripherals) with the user application. The application support layer (APS) and the application programming interface allow the user to control the sensor network and to handle the communication between the devices. In addition, the APS layer specifies what kind of device the hardware is (e.g., coordinator, router, or end device). The media access control layer based on the IEEE 802.15.4 standard operates on top of the physical layer (PHY) and is responsible for the routing within the network. The PHY layer comprises not only the transceiver but also the sensors and energy source (Kuorilehto et al., 2007). The user application is a program developed by the user to configure the sensor network and to realize advanced functionalities (e.g., logging function, sensor drivers, etc.).

The wireless sensor network technology allows real-time SWC monitoring at unprecedented spatial and temporal resolution for observing hydrologic processes in small watersheds (0.1–80 km^2). A well-designed wireless sensor network can be infinitely expanded and can be dynamically adapted. In addition, it can react to external influences. For example, a SWC sensor network can be linked to an automated rain gauge and the sampling frequency

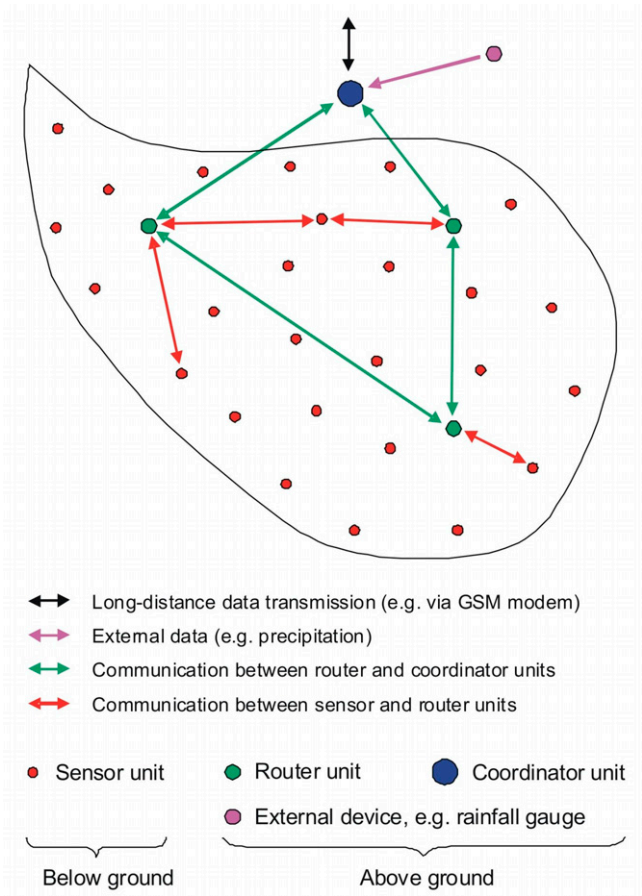

Fig. 1. The reactive hybrid WUSN topology of SoilNet exemplified for a virtual catchment area.

could be increased during rainfall events to allow the investigation of highly dynamic processes. A major advantage of long-term sensor network measurements compared with traditional ground-based SWC measurement campaigns (e.g., Famiglietti et al., 2008) is that the SWC sensors remain in the soil for a long period of time. Thus, comparisons between different points in time are not affected by different measurement positions or changes in probe characteristics (e.g., different calibration quality). In addition, sensor networks enable area-differentiated continuous monitoring of soil water profiles. Such data are valuable for hydrologic model evaluation (e.g., Zehe et al., 2005) and to improve the prediction of hydrologic fluxes using data assimilation (Vereecken et al., 2008).

Besides these advantages of wireless sensor networks, a considerable disadvantage is their strong reliance on batteries. Even for sensors with low power consumption, the batteries have to be changed after several years. This will lead to additional maintenance costs and should be considered when using sensors in the subsurface. Therefore, sensor selection should also consider energy consumption to ensure a long battery life. Finally, wireless transmission may be more prone to signal transmission failures(e.g., attenuation, radio interference, dead battery), which implies a risk of data loss. This can largely be avoided with appropriate communication protocols, but it cannot be completely excluded. A solution to this problem would be to store data locally on each sensor unit so that data could still be recovered in the case of transmission failure (Trubilowicz, 2009).

Akyildiz and Stuntebeck (2006) suggested two possible topologies for wireless underground sensor networks: the underground topology and the hybrid topology. In the underground topology, all sensor devices are deployed underground expect for the coordinator unit. Akyildiz and Stuntebeck (2006) presented several reasons to use a wireless underground topology in the case where subsurface properties like SWC have to be monitored (e.g., concealment, ease of deployment, reliability, and coverage density). A recent wireless underground topology was presented by Ritsema et al. (2009). The hybrid topology is a mixture of underground and aboveground devices. The choice of network topology is important for network reliability as well as for power conservation. Li et al. (2007) and Bogena et al. (2009) showed that the maximum achievable separation to allow communication between underground sensors can be as low as 5 m under unfavorable soil conditions. This implies that underground topologies need a high sensor density or require considerable power to overcome soil attenuation. Such high sensor density and power consumption are prohibitive for many of the envisioned applications of wireless SWC sensor networks.

Therefore, a hybrid wireless underground sensor network topology, which is composed of a mixture of underground end devices each wired to several soil sensors and aboveground router devices, is preferable to achieve longer transmission ranges (Bogena et al., 2009). A schematic of a hybrid topology is shown in Fig. 1. The hybrid topology allows data to be routed out of the underground in a few steps, thus reducing the underground travel distance to save power. Principally, an underground end device can communicate with all router devices within the hybrid topology but it will effectively only use the nearest routers because these will typically have the highest signal strength.

Materials and Methods

The SoilNet Wireless Network Technology

SoilNet is a wireless underground sensor network for monitoring SWC at the catchment scale. It was developed at the Forschungszentrum Jülich using the proprietary, license-free, protocol stack JenNet (Jennic Ltd., 2009a). Similar to ZigBee, JenNet is based on the IEEE 802.15.4 specification optimized for short-range wireless networking applications. To minimize energy consumption, the data communication rate is reduced compared with a wireless local-area network (250 kbit s^{-1} instead of 54 Mbit s^{-1}) and is thus especially suited for battery-operated wireless network applications. The kernel of the communication hardware is the ZigBee-compliant, high-power, wireless module JN5139 (Jennic Ltd., 2009b). It uses the unlicensed 2.4-GHz band and supports star, tree, and linear topologies (network sizes up to 250 nodes in a tree and 1000 nodes in a linear topology). Further information on the SoilNet technology can be found at the SoilNet website (Forschungszentrum Jülich, 2009).

SoilNet Soil Water Content Sensors

There are several factors that have to be considered when selecting a sensor for network applications. To maximize the lifetime of a sensor network, the sensors have to be very economic concerning energy use and should be reasonably robust. Because of the multitude of measurements within the sensor network, the interpretation of the sensor signal has to be straightforward and unambiguous. In addition, to maximize the number of sensor nodes, the sensors have to be as inexpensive as possible. Because capacitance sensors are relatively inexpensive and easy to operate, they seem to be a promising choice for SWC measurements with sensor networks.

The capacitance method is a widely used electromagnetic technique for SWC estimation (Blonquist et al., 2005). Bogena et al. (2007) and Rosenbaum et al. (2010) evaluated the low-cost capacitance sensor ECH_2O EC-5 (Decagon Devices, Pullman, WA) and came to the conclusion that this sensor is appropriate for sensor network applications. The ECH_2O sensor circuitry measures the dielectric permittivity of the material surrounding a thin, fiberglass-enclosed probe at a frequency of 70 MHz. A detailed description of the measurement principle of this sensor was provided in Bogena et al. (2007). The sensor output is related to SWC using a two-step approach.

The first step involves the determination of the apparent permittivity (K_a) using appropriate output voltage–permittivity relations. Rosenbaum et al. (2010) proposed the following functional relationship:

$$\sqrt{K_a} = av^b + c \quad [1]$$

where v is the sensor response and a, b, and c are fitting parameters. Equation [1] is derived from a model detailed in Robinson et al. (2005) and Sakaki et al. (2008). We used a single set of fitting parameters for each sensor type, as proposed by Rosenbaum et al. (2010), based on an analysis of 105 EC-5 sensors and resulting in a mean error of about 1.6% (v/v). Given the large sensor-to-sensor variability observed by Rosenbaum et al. (2010), we evaluated each EC-5 sensor in a sand bed with a known SWC. All sensors that showed significant deviations (>5% v/v) from the known water content were not considered for field installation. Bogena et al. (2007) showed that the EC-5 sensor was sensitive to temperature and bulk electrical conductivity changes. Because the EC-5 sensor does not measure these parameters, sensor responses were not corrected for temperature and conductivity effects; however, laboratory experiments demonstrated that the EC-5 does not show large temperature variations because the temperature effects on the sensor are offset by the permittivity changes of the soil water (unpublished data, 2010). Furthermore, the bulk conductivity of the topsoil in the Wüstebach catchment is generally low (<0.1 dS m^{-1}) and laboratory experiments showed that corrections are of minor importance in this conductivity range (unpublished data, 2010).

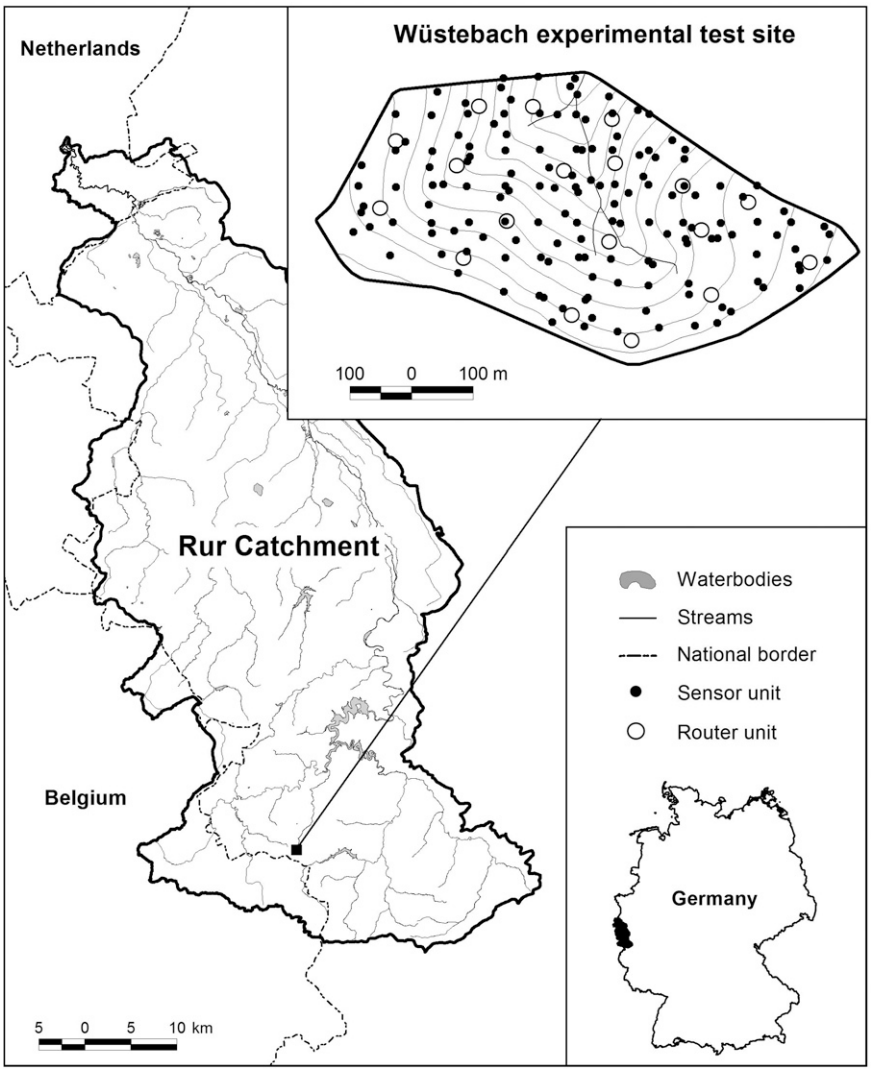

Fig. 2. Location of the experimental Wüstebach catchment within the TERENO Rur/Lower Rhine Valley observatory and the SoilNet instrumentation (sensor and router units); the contour interval is 3 m.

In a second step, the SWC, θ (m^3 m^{-3}), can be calculated using the empirical relation derived by Topp et al. (1980):

$$\theta = -5.3\times10^{-2} + 2.92\times10^{-2} K_a - 5.5\times10^{-4} K_a^2 + 4.3\times10^{-6} K_a^3 \quad [2]$$

When additional soil parameters are available (e.g., bulk soil density), the use of a semiempirical dielectric mixing model to determine the SWC can be considered (e.g., Roth et al., 1990).

The Wüstebach Experimental Test Site

The Wüstebach experimental test site is a small subcatchment of the River Rur basin and part of the TERENO Eifel/Lower Rhine Valley Observatory (Fig. 2). The Wüstebach test site covers an area of 27 ha and is situated in the German low mountain ranges within the National Park Eifel. The mean annual precipitation (1979–1999) is 1220 mm. The bedrock is composed of Devonian shales with occasional sandstone inclusions. The geomorphology is plateau like with a mean slope of 3.6% and a maximum slope of 10.4%. The soils developed on periglacial solifluction layers, with an average thickness of approximately 1 to 2 m. Mainly Cambisols are found on the hillslopes, while gleyic soils and half-bogs have developed near the river. The soil texture is loamy silt. The main vegetation type is Norway spruce [*Picea abies* (L.) H. Karst.], with coverage of about 90%.

The SoilNet instrumentation of the Wüstebach test site is part of the TERENO activity (TERENO, 2010) and was accomplished in close cooperation with the DFG/TR32 (Transregional Centre 32, 2009). In late 2008, we started with the installation of SoilNet

at the Wüstebach site. The instrumentation was completed in August 2009, with a total number of 600 EC-5 sensors and 300 5TE sensors (Decagon Devices) at 150 locations (a combination of 50 sensor units in a 60- by 60-m raster and 100 randomly distributed sensor units) and three depths (5, 20, and 50 cm). We installed two sensors at each depth with a separation of 5 cm to increase the measurement volume and to enable the examination of inconsistencies (e.g., imperfect contact of sensors to the soil matrix). At the 5- and 50-cm depths, one EC5 and one 5TE sensor were installed, whereas two EC-5 sensors were installed at the 20-cm depth. For each of the 150 sensor unit locations, we used a manual twist drill to produce a borehole of 0.2-m diameter. The SWC sensors were installed horizontally into the soil. A special pilot blade was required to prepare insertion holes for the sensor. The pilot blades were machined somewhat thinner than the actual sensors to avoid air gaps. Contact with the soil matrix was assured by comparing the outputs of two adjacent SWC sensors. In case the difference in SWC was >5% (v/v), the position of the sensors was changed until the difference in SWC is <5%. From August to November 2009, more than six million SWC measurements were made and stored in a central database with a measurement frequency of 15 min.

Analysis of Spatial Variability and Topographic Controls of Soil Water Content Distribution

The main goal of this study was to evaluate the potential of wireless sensor networks for the examination of SWC variation at the catchment scale. We inspected the data taken between August and November 2009 and excluded inconsistent measurements using the following procedure. First, the plausibility of the SWC time series was visually evaluated by plotting all sensors for a single depth. Sensors with SWC time series that did not show the expected dynamics in response to rainfall were discarded. Second, the duplicate measurements between sensors installed with a 5-cm separation in a single depth were qualitatively evaluated. If differences were estimated to be >10% (v/v), both measurement time series were also discarded. Finally, only time series were considered that were complete for the entire analysis period to avoid variations in the number of sampling sites between different dates. In the following, we have focused on an analysis of the variance and spatial correlation of the mean daily SWC. Therefore, we averaged the 15-min SWC data to obtain daily mean values.

Recent studies have shown that the sensor characteristics and the associated measurement errors are different for the EC5 and 5TE sensors (Rosenbaum et al., 2010). To avoid complications due to these different sensor characteristics, we decided to focus on the measurements of the EC5 sensors in this study. Using the simple but strict preprocessing approach outlined above, we obtained a data set consisting of 108 out of 150 sampling sites and 432 out of 600 EC-5 sensors. This high failure rate can be considerably reduced with more advanced processing; however, this will lead to an uneven number of sampling sites per measurement time, which we considered unwanted for the present analysis.

Famiglietti et al. (2008) proposed the SD, CV, and skewness as the most suitable statistical parameters for the analysis of SWC variability as a function of mean surface SWC. The SD, CV, and skewness were calculated using all the available daily measurements every 3 to 4 d covering the whole test site and measurement period (20 times) for three depths (5, 20, and 50 cm). Since the difference between the mean of the two EC-5 sensors installed at the 20-cm depth was only 0.3% (v/v), we used the average of the two sensors in this study.

It was expected that lateral subsurface flow occurs because the basal percolation is restricted due to the geologic and pedologic characteristics of the Wüstebach catchment. In such a case, the pattern of SWC cannot be understood simply by considering vertical flow in the soil profile (Burt and Butcher, 1985). To evaluate the potential of wireless sensor networks for the analysis of topographic controls on SWC patterns, we used three basic topographic parameters: elevation, slope, and wetness index (WI). The WI is essentially the log-transformed topographic index (area upslope divided by the local hillslope gradient) proposed by Beven and Kirkby (1979). We calculated the WI using the ArcView extension developed by Schmidt (2002), including an additional smoothing filter. For the calculation of these parameters, we used a digital elevation model with a resolution of 10 m. For each sampling time, soil depth, and topographic parameter, we calculated the R^2, which was then plotted against the mean SWC content.

Geostatistical Analysis

The usefulness of kriging methods for the regionalization of SWC data at the catchment scale has already been demonstrated (e.g., Bárdossy and Lehmann, 1998; Herbst and Diekkrüger, 2003; Herbst et al., 2006). External drift kriging is well suited to include additional information in the kriging procedure (e.g., Snepvangers et al., 2003), and we used multiple linear regression to consider additional topographic information.

Multiple Linear Regression

In multiple linear regression, p independent variables (i.e., elevation, slope, and WI) are related to a single dependent variable (i.e., SWC) for n observations:

$$y_i = \beta_0 + \sum_j^p \beta_j x_{i,j} \quad [3]$$

where, for the ith of n observations, y_i is the dependent variable and $x_{i,1}, \ldots, x_{i,p}$ are the independent variables. The unknown regression coefficients $\beta_0, \ldots, \beta_p$ are determined using a least squares approach. Frequently, the R^2 value is used to quantify the variability of

the dependent variable that is explained by the variation in the independent variables:

$$R^2 = 1 - \frac{\mathrm{SSE}}{\mathrm{SST}} \quad [4]$$

where SSE is the sum of squared errors and SST is the total sum of squares. Using the R^2 as the criterion for linear regression model selection, however, has the disadvantage of R^2 increasing with each additional variable included in the regression. A more appropriate criterion is the adjusted coefficient of determination, $R_{\mathrm{adj}}{}^2$, which corrects the explained variability for the number of parameters:

$$R^2_{\mathrm{adj}} = 1 - \left(1 - R^2\right)\frac{n-1}{n-p-1} \quad [5]$$

Akaike (1973) introduced an alternative to $R_{\mathrm{adj}}{}^2$, which is now known as the Akaike information criterion (AIC). This measure can be used to select an optimum model in terms of the SSE and the number of parameters involved:

$$\mathrm{AIC} = n\log_e\left(\frac{\mathrm{SSE}}{n}\right) + 2p \quad [6]$$

A small AIC indicates an optimum regression model close to the "true" model. In this study, model selection was based on a stepwise regression technique in which variables were added one at a time to the model as long as the significance of the added parameter remained below a specified significance level α (Deutsch and Journel, 1998).

Variography and Kriging

Spherical variogram functions were fitted to the experimental variogram:

$$\gamma(h) = \begin{cases} c_0 + c_1\left[1.5\dfrac{h}{a} - 0.5\left(\dfrac{h}{a}\right)^3\right] & \text{for } h \le a \\ c_0 + c_1 & \text{for } h > a \end{cases} \quad [7]$$

where h is the separation distance, c_0 is the nugget, c_1 is the sill, and a is the spatial autocorrelation range. Kriging estimates are a weighted mean of the neighboring sampling location values. The weights λ_i are chosen according to the semivariance γ as a function of distance h (Eq. [7]) between prediction location x and the neighboring sampling location values x_j:

$$\begin{cases} \displaystyle\sum_{i=1}^{n}\lambda\gamma\left(x_j - x_i\right) + \mu = \gamma\left(x_j - x\right) \quad j = 1,\ldots,n \\ \displaystyle\sum_{i=1}^{n}\lambda = 1 \end{cases} \quad [8]$$

where μ is the Lagrange parameter. Ordinary kriging was extended to external drift kriging by Ahmed and DeMarsily (1987). In this study, a covariable $Y(x)$ was assumed to be linearly related to the target variable. To minimize the estimation variance with this assumption, the linear equation system was modified to

$$\begin{cases} \displaystyle\sum_{i=1}^{n}\lambda_i\gamma\left(x_j - x_i\right) + \mu_1 + \mu_2 Y\left(x_j\right) = \\ \qquad\qquad \gamma\left(x_j - x\right) \qquad j = 1,\ldots,n \\ \displaystyle\sum_{i=1}^{n}\lambda_i = 1 \\ \displaystyle\sum_{i=1}^{n}\lambda_i Y\left(x_i\right) = Y\left(x\right) \end{cases} \quad [9]$$

with the Lagrange parameters μ_1 and μ_2. We applied the KT3D routine of the Geostatistical Software Library (Deutsch and Journel, 1998) to perform ordinary and external drift kriging.

To quantify the improvement of using covariates in the estimation, a cross-validation was performed. In cross-validation, the prediction performance is evaluated by leaving out data points one at a time and estimating the properties of the location from the covariables and the neighboring data. This allows the error between the measurements and the estimation to be computed for every sample location. The mean absolute error between estimates and measurements was computed. Furthermore, the RMSE was computed according to

$$\mathrm{RMSE} = \sqrt{\frac{1}{n}\mathrm{SSE}} \quad [10]$$

Results and Discussion

Analysis of Spatial Variability

The temporal changes in daily mean SWC at the 5-, 20-, and 50-cm depth from August 2009 to November 2009 are presented in Fig. 3. Due to the relatively wet conditions during this period, the lowest measured SWC was 28.3% (v/v). The SWC range of the SoilNet data is smaller (~12% (v/v)) than previous studies because of the shorter period of time. The CV, SD, and skewness are presented as a function of the mean SWC in Fig. 4. A comparison of the 5-cm SoilNet data with other published results indicated that the observed SWC variability in this study was relatively high. For example, the 800-m-scale data described in Famiglietti et al. (2008) showed a mean SD of ~5% (v/v). The data of Famiglietti et al. (2008), however, were obtained in flat areas where there was no topographical effect on SWC patterns. The Tarrawarra data set analyzed by Western et al. (1999) has a maximum SD of ~5% (v/v). This site is smaller than the Wüstebach site, however, and the increase in the SD with increasing scale is well established (e.g., Famiglietti et al., 2008). In addition, the lower SWC variability of the Tarrawarra site is probably related to the land use (pasture instead of forest). The results presented here correspond well with those of Grant et al. (2004), who also found SD values up to 12% (v/v) in a mountainous site of comparable size (36 ha).

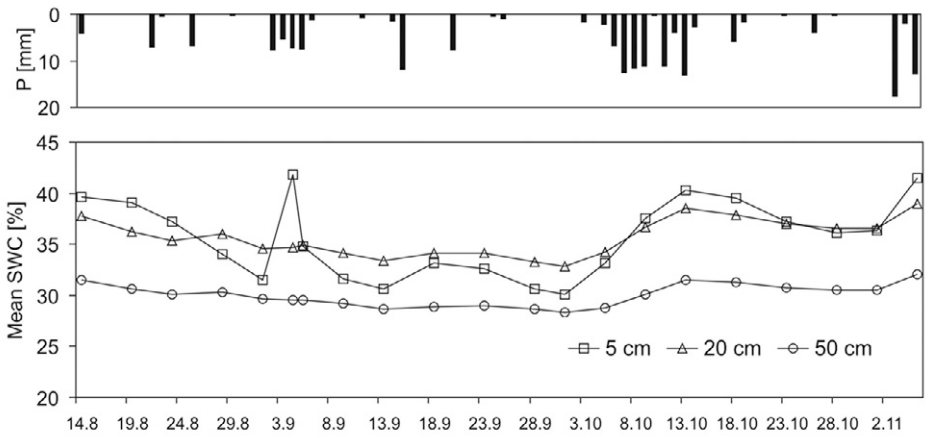

Fig. 3. Time series of daily precipitation (P) and mean soil water contents (SWC) measured at 5-, 20-, and 50-cm depths.

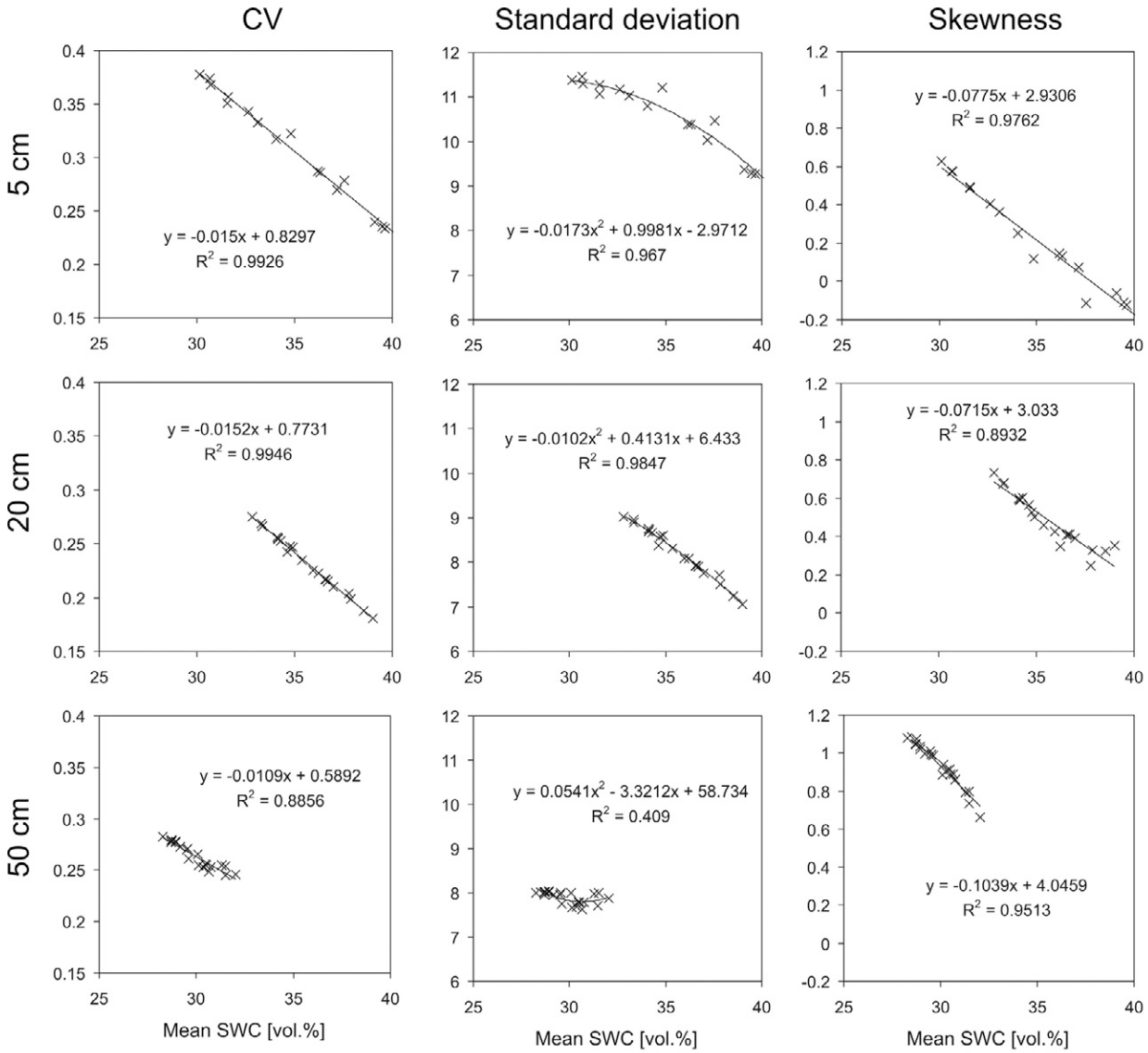

Fig. 4. Coefficient of variation, SD, and skewness vs. mean soil water content (SWC) for 5-, 20-, and 50-cm soil depths as well as empirical linear and polynomial fitting functions.

The most striking aspect of the SoilNet data is the low scattering of the relationships presented in Fig. 4, which is also reflected in the high R^2 for the empirical linear and polynomial functions that were fitted. The scatter shown in Fig. 4 is considerably less than the scatter observed in similar surface SWC variability studies using discontinuous ("campaign-type") measurements. Famiglietti et al. (1998, Fig. 3) presented the variance of topsoil SWC as a function of the mean SWC along a 200-m transect. Their results showed considerable scattering for SWC values above 20% (v/v). The results of Seyfried (1998, Fig. 5) also showed considerable scattering in the SWC variability of the topsoil within three headwater catchments similar in size to the Wüstebach catchment. The SWC data from the Tarrawarra catchment presented by Western et al. (1999, Fig. 4) also showed large scattering, especially for intermediate and dry soils. In comparison with the SoilNet data, this significant scattering in SWC variability is related to the lower number of measurement sites and the discontinuous ("campaign-style") acquisition strategy. Such monitoring strategies may introduce additional variability due to variations in sampling locations and measurement devices (e.g., calibration variances, sensor abrasion, sensor-to-sensor variability, etc.).

The SWC range of the 20-cm SoilNet data is significantly lower (6% [v/v]) but shows a similar pattern as the 5-cm data. Because the soil water at 20 cm has a longer travel time than at 5 cm, part of the spatial variability might be removed through lateral redistribution or root water uptake. The SWC range of the 50-cm SoilNet data is even lower than at 20 cm (~4% [v/v]). In addition, the range of the SD is much less, and no clear correlation with the mean SWC exists. This indicates that factors controlling the longer travel time of the soil water at 50 cm lead to a larger reduction in spatial variability by soil water redistribution processes or that

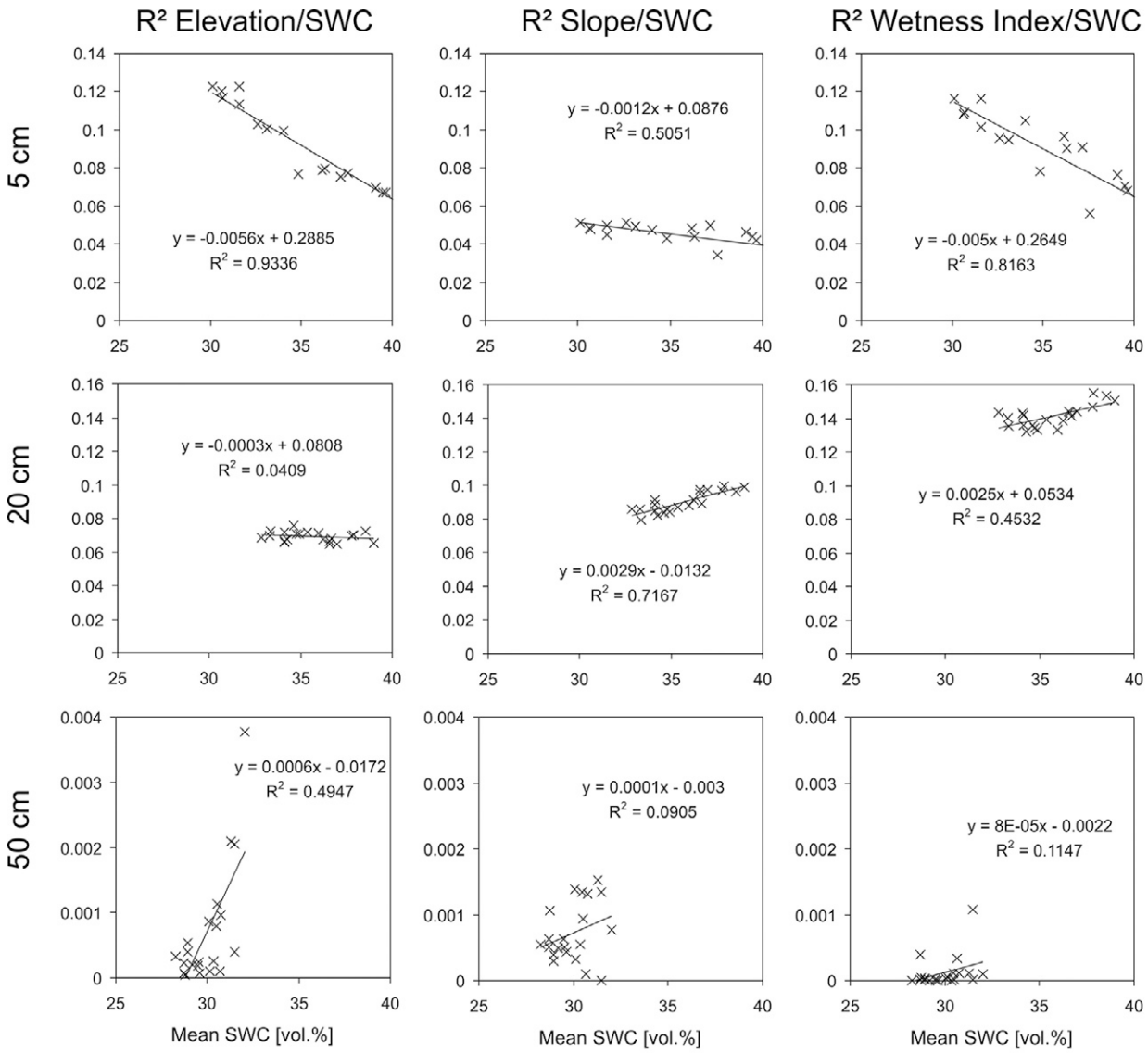

Fig. 5. The R^2(elevation/soil water content [SWC]), R^2(slope/SWC), and R^2(wetness index [WI]/SWC) vs. mean SWC for 5-, 20-, and 50-cm soil depths as well as empirical linear and polynomial fitting functions.

the subsurface is less heterogeneous. To test these assumptions, a simulation of soil water transport using a three-dimensional hydrologic model is needed.

It is evident that the reduced scatter in the type of relationships presented in Fig. 4 is beneficial for interpreting and understanding the processes generating spatial SWC variability. For example, the scaling method proposed by Vereecken et al. (2007) can now be evaluated with more rigor. It has to be noted, however, that several factors may have influenced this finding. For instance, upscaling of the 15-min SWC data into daily averages may have decreased the variability although changes in SWC, especially in the deeper soil, are rather slow. Furthermore, the range in the observed SWC is lower than in other studies (e.g., Famiglietti et al., 1998, 2008). This may also have contributed to the lower scattering, because SWC variability tends to decrease near the dry and wet ends of the mean SWC (Vereecken et al., 2007).

Table 1. Variogram parameters nugget (c_0), sill (c_1), and range (a_1). The regression equations for water content (θ) are given, where h_r is the relative elevation of the terrain, WI is the wetness index, and β is terrain slope. Goodness-of-fit is given in terms of the coefficient of determination (R^2), the adjusted coefficient of determination (R_{adj}^2) and the Akaike information criterion (AIC).

Date	n	c_0	c_1	a_1	Regression	R^2	R_{adj}^2	AIC
		— %² (v/v) —		m				
1 Oct. 2009	133	55.4	76.5	131.8	θ = 297.4 – 0.53hr + 7.88WI	0.228	0.216	611.6
11 Oct. 2009	129	53.3	25.6	157.8	θ = 272.0 – 0.36hr – 1.66β	0.132	0.118	546.9

Figure 5 presents correlations between the basic topographic parameters of elevation, slope, and WI with SWC plotted against the mean SWC. The 5-cm data show the highest R^2 for elevation and WI (mean R^2 = 0.088 and 0.087, respectively), whereas the mean R^2 for slope is considerably lower (0.045). Interestingly, for the 20- and 50-cm data sets, the mean R^2 for elevation is smaller than the R^2 for slope and WI, again indicating the effect of soil water redistribution.

Despite the weak correlations between the topographic parameters and the SWC, there are strong correlations between R^2(elevation/SWC), R^2(slope/SWC), and R^2(WI/SWC) and the mean SWC. Topographic features are correlated more strongly with SWC when the SWC is intermediate. This indicates that the control of topographic features on the SWC pattern depends on the soil water status. Interestingly, this effect is less observable for the 20- and 50-cm data, which might also be due to the smaller SCW range at these measurement depths.

Geostatistical Analysis

The variogram parameters in Table 1 reveal a higher structural and total semivariance and a lower range for the drier measurement day (1 Oct. 2009) than the wetter measurement day (11 Oct. 2009). Both variograms have approximately the same nugget effect (Fig. 6), which indicates that the sum of the subscale variability and the measurement error did not change. The lower spatial variability for the wet situation has been reported in a number of studies (e.g., Famiglietti et al., 1998). It has been attributed to the saturated SWC, which poses an upper limit and is typically not strongly variable in headwater catchments with relatively homogeneous soils (Vereecken et al., 2007).

The variograms shown in Fig. 6 can be used to investigate the scaling behavior of soil moisture variance with increasing support scale. The functional relationship between variance and support scale can be derived using the regularization procedure presented by Journel and Huijbregts (1978) and Western and Blöschl (1999). The idea of regularization is to obtain the properties of an averaged process by running a linear filter over the original point process. The variance of the averaged process for a given support scale is the total variance minus the variance within the support scale. The variance within the support scale is calculated using the variogram and a probability density function of the distances between two points within the support (Western and Blöschl, 1999, Appendix). Figure 7 presents the scaling behavior of the logarithmic variance plotted

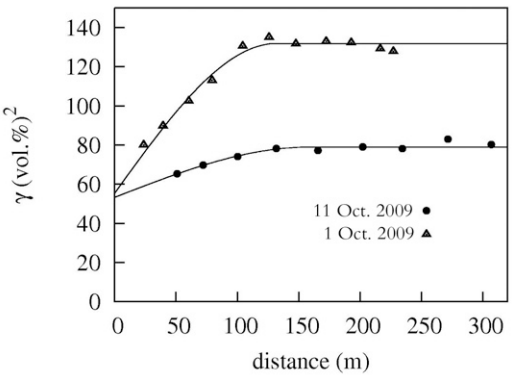

Fig. 6. Variograms for the drier (1 Oct. 2009) and wetter (11 Oct. 2009) soil water content (SWC) measurement dates.

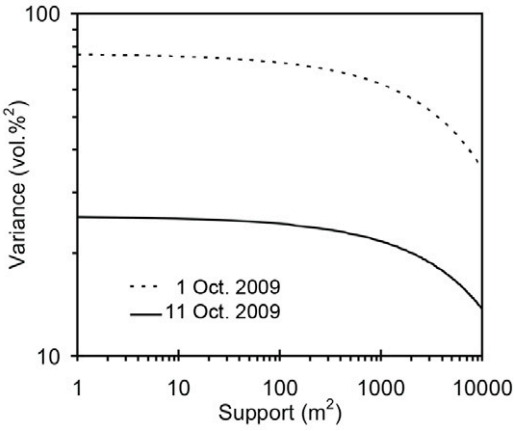

Fig. 7. Soil water content variance vs. support scale for the drier (1 Oct. 2009) and wetter (11 Oct. 2009) soil water content (SWC) measurement dates.

against the logarithmic support scale. Rodriguez-Iturbe et al. (1995) found a linear relationship with a slope of −0.2 for such a plot. In this study, logarithmic variances showed a fairly linear trend until the support scale reached 1000 m^2, approximately a 32-m length scale. For larger scales, there was a noticeable nonlinearity in the scaling for both dates. The slope of the relationship is approximately −0.03 for a support scale of <1000 m^2, which is higher than that found by Rodriguez-Iturbe et al. (1995). The shape of the scaling relationship found in our study is similar to the larger scale results of Ryu and Famiglietti (2006), especially for their Case 1, which was also based on a spherical variogram model. This indicates that the type of variogram model has a strong impact on the shape of these scaling relationships. Unfortunately, there is quite some uncertainty and subjectivity in selecting an appropriate variogram model, which should be remembered when using these scaling relationships (e.g., Crow and Wood, 2002).

Figure 8 shows the interpolated maps of SWC for the dry and wet measurement dates using ordinary kriging (OK) and external drift kriging (EDK). For both the dry and the wet days, OK clearly showed the wetter valley bottom close to the drainage network. This indicates that the high sampling density that can be achieved with wireless sensor networks allows the basic pattern of SWC distribution in the catchment to be captured.

The ancillary data for EDK were selected using a stepwise regression procedure. For the drier date, the stepwise regression procedure selected relative elevation and the WI as covariates. They also provided the lowest AIC (Table 1); however, the R^2 was low. As expected, the regression coefficients indicate a negative relation between SWC and elevation (i.e., the lower parts of the terrain show the highest SWC) and a positive relation between the WI and SWC. For the wet date, elevation was selected again, but this time in combination with terrain slope. The R^2 for the wet date is even lower than for the dry date. The use of these covariates in EDK sharpens the SWC pattern and increases variability compared with OK (Fig. 8). The cross-validation procedure showed a small but consistent increase in estimation accuracy when using EDK (Table 2). Prediction accuracy was lower for the dry date because the variability in SWC was higher for that date.

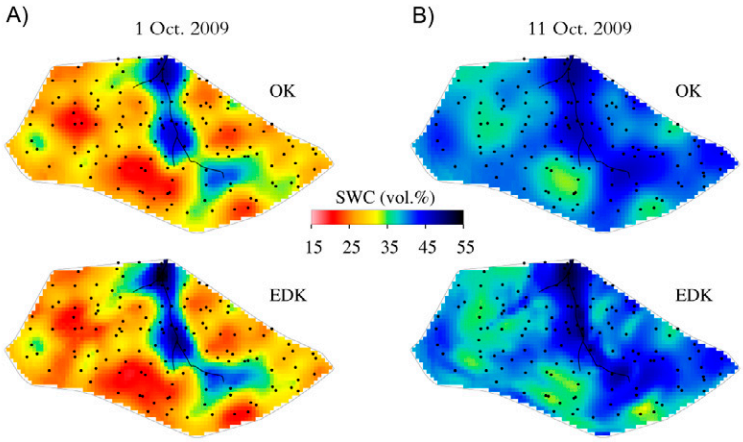

Fig. 8. Interpolated maps of soil water content (SWC) for the (A) drier and (B) wetter measurement dates using ordinary kriging (OK) and external drift kriging (EDK).

Table 2. Cross-validation result in terms of mean absolute error (MAE) and root mean square error (RMSE) for ordinary kriging (OK) and external drift kriging (EDK).

	OK		EDK	
Date	MAE	RMSE	MAE	RMSE
	% (v/v)			
1 Oct. 2009	8.62	10.32	8.58	10.25
11 Oct. 2009	6.92	8.29	6.75	8.24

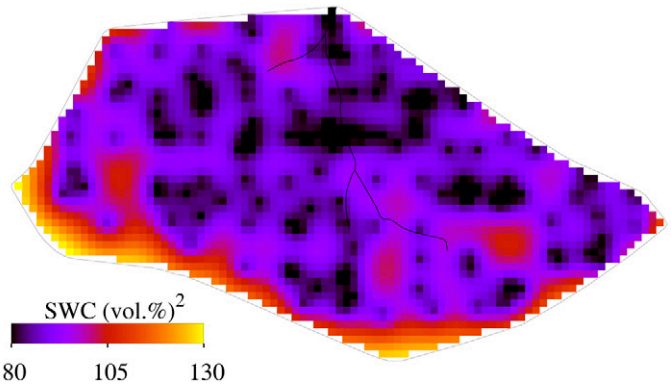

Fig. 9. Kriging variance using ordinary kriging for the data of 1 Oct. 2009; high soil water content (SWC) values indicate areas where a reduction in estimation error can be achieved by adding additional sensor nodes.

One way to further reduce spatial estimation errors is to investigate additional covariables that show a close link to SWC, like soil properties or stand age. Another way to reduce spatial estimation error would be to add measurement nodes to the network. In this context, the use of the kriging variance may be helpful. Figure 9 shows an example of the kriging variance using OK for the data of 1 Oct. 2009. The red and brown patches indicate areas that show potential to improve the spatial coverage of the SWC sensor network. Of course, the highest kriging variance is found close the catchment boundary. The reduction in estimation error when adding additional nodes can be estimated using the kriging procedure. Because sensor networks are very flexible, optimization of the network (e.g., by rearranging or adding sensor nodes) can be easily accomplished.

Conclusions

This study has shown the applicability of the SoilNet wireless sensor network for the analysis of SWC patterns at the headwater catchment scale. From August to November 2009, more than six million measurements were taken. This shows that the wireless underground sensor network concept can be successfully applied in forested, low-mountainous, headwater catchments. A statistical analysis of the SoilNet data showed that the observed SWC variability in this study was relatively high, but corresponds well with the SWC variability found by Grant et al. (2004) in a mountainous region. The sensor network data showed less scatter than similar studies based on discontinuous SWC measurements. This indicates that sensor networks allow more detailed insights into the processes generating SWC variability. The variability in SWC at the 50-cm depth was significantly lower than at 5 cm, suggesting that factors controlling the longer travel time reduce the spatial variability of the SWC. Topographic features showed the strongest correlation with SWC during dry periods, indicating that the control of topography on the SWC pattern depends on the soil water status. Interpolation results indicated that the high sampling density allowed the key patterns of SWC variation in the catchment to be captured. Future work will focus on the upscaling of point measurements to larger scales (e.g., using SoilNet data for the validation of remote-sensing-based SWC estimations or distributed hydrologic model results) and the analysis of spatiotemporal SWC variation at short time scales (<1 d).

Acknowledgments

We gratefully acknowledge financial support by the SFB/TR32 "Pattern in Soil–Vegetation–Atmosphere Systems: Monitoring, Modelling, and Data Assimilation" funded by the Deutsche Forschungsgemeinschaft (DFG) and by TERENO "Terrestrial Environmental Observatories" funded by the Federal Ministry of Education and Research (BMBF).

References

Ahmed, S., and G. DeMarsily. 1987. Comparison of geostatistical methods for estimating transmissivity using data on transmissivity and specific capacity. Water Resour. Res. 23:1717–1737.

Akaike, H. 1973. Information theory and an extension of the maximum likelihood principle. p. 267–281. *In* B.N. Petrov and F. Csaki (ed.) Int. Symp. on Inf. Theory, 2nd, Tsahkadsor, Armenia. 25–29 June. Akademiai Kiado, Budapest.

Akyildiz, I.F., and E.P. Stuntebeck. 2006. Wireless underground sensor networks: Research challenges. Ad Hoc Networks 4:669–686.

Bárdossy, A., and W. Lehmann. 1998. Spatial distribution of soil moisture in a small catchment: 1. Geostatistical analysis. J. Hydrol. 206:1–15.

Beven, K.J., and M.J. Kirkby. 1979. A physically based variable contributing area model of basin hydrology. Hydrol. Sci. Bull. 24:43–69.

Blonquist, J.M., Jr., S.B. Jones, and D.A. Robinson. 2005. Standardizing characterization of electromagnetic water content sensors: 2. Evaluation of seven sensing systems. Vadose Zone J. 4:1059–1069.

Bogena, H.R., J.A. Huisman, H. Meier, U. Rosenbaum, and A. Weuthen. 2009. Hybrid wireless underground sensor networks: Quantification of signal attenuation due to soil adsorption. Vadose Zone J. 8:755–761.

Bogena, H.R., J.A. Huisman, C. Oberdörster, and H. Vereecken. 2007. Evaluation of a low-cost soil water content sensor. J. Hydrol. 344:32–42.

Bogena, H., K. Schulz, and H. Vereecken. 2006. Towards a network of observatories in terrestrial environmental research. Adv. Geosci. 9: 109–114.

Burt, T.P., and D.P. Butcher. 1985. Topographic controls of soil moisture distributions. J. Soil Sci. 36:469–486.

Cardell-Oliver, R., K. Smettem, M. Kranz, and K. Mayer. 2005. A reactive soil moisture sensor network: Design and field evaluation. Int. J. Distrib. Sens. Networks 12:149–162.

Crow, W.T., and E.F. Wood. 2002. The value of coarse-scale soil moisture observations for regional surface energy balance modeling. J. Hydrometeorol. 3:467–482.

Deutsch, C.V., and A.G. Journel. 1998. GSLIB: Geostatistical Software library and user's guide. 2nd ed. Oxford Univ. Press, New York.

Digi International. 2010. XBee/XBee-PRO ZB RF modules. Digi Int., Minnetonka, MN.

Famiglietti, J.S., J.W. Rudnicki, and M. Rodell. 1998. Variability in surface moisture content along a hillslope transect: Rattlesnake Hill, Texas. J. Hydrol. 210:259–281.

Famiglietti, J.S., D. Ryu, A.A. Berg, M. Rodell, and T.J. Jackson. 2008. Field observations of soil moisture variability across scales. Water Resour. Res. 44:W01423, doi:10.1029/2006WR005804.

Forschungszentrum Jülich. 2009. SoilNet. Available at www.fz-juelich.de/icg/icg-4/index.php?index=739 (verified 31 May 2010). Forschungszentrum Jülich, Jülich, Germany.

Grant, L., M. Seyfried, and J. McNamara. 2004. Spatial variation and temporal stability of soil water in a snow-dominated, mountain catchment. Hydrol. Processes 18:3493–3511.

Grayson, R.B., A.W. Western, F.H.S. Chiew, and G. Blöschl. 1997. Preferred states in spatial soil moisture patterns: Local and non-local controls. Water Resour. Res. 33:2897–2908.

Herbst, M., and B. Diekkrüger. 2003. Modelling the spatial variability of soil moisture in a micro-scale catchment and comparison with field data using geostatistics. Phys. Chem. Earth 28:239–245.

Herbst, M., B. Diekkrüger, and H. Vereecken. 2006. Geostatistical co-regionalization of soil hydraulic properties in a micro-scale catchment using terrain attributes. Geoderma 132:206–221.

Jennic Ltd. 2009a. Product brief– JenNet protocol stack. Available at www.jennic.com/products/protocol_stacks/jennet (verified 31 May 2010). Jennic Ltd,, Sheffield, UK.

Jennic Ltd. 2009b. Product brief—JN5139-xxx-Myy: IEEE802.15.4/ZigBee module family. Available at www.jennic.com/files/product_briefs/JN5139-xxx-Myy-PB_v1.2.pdf (verified 31 May 2010). Jennic Ltd., Sheffield, UK.

Journel, A.G., and C.J. Huijbregts. 1978. Mining Geostatistics. Elsevier, New York.

Kuorilehto, M., M. Kohvakka, J. Suhonen, P. Hämäläinen, M. Hännikäinen, and T.D. Hamalainen. 2007. Ultra-low energy wireless sensor networks in practice: Theory, realization, and deployment. John Wiley & Sons, Chichester, UK.

Li, L., M.C. Vuran, and I.F. Akyildiz. 2007. Characteristics of underground channel for wireless underground sensor networks. *In* Med Hoc Net 2007: Proc. Annu. Mediterranean Ad Hoc Networking Workshop, 6th, Corfu, Greece. 12–15 June 2007. Available at di.ionio.gr/medhocnet07/wp-content/uploads/papers/220.pdf (verified 31 May 2010). Ionian Univ., Corfu, Greece.

Löw, A., R. Ludwig, and W. Mauser. 2006. Derivation of surface soil moisture from ENVISAT ASAR wide swath and image mode data in agricultural areas. IEEE Trans. Geosci. Remote Sens. 444:889–899.

Ritsema, C.J., H. Kuipers, L. Kleiboer, E. van den Elsen, K. Oostindie, J.G. Wesseling, J.-W. Wolthuis, and P. Havinga. 2009. A new wireless underground network system for continuous monitoring of soil water contents. Water Resour. Res. 45:W00D36, doi:10.1029/2008WR007071.

Robinson, D.A., C.S. Campbell, J.W. Hopmans, B.K. Hornbuckle, S.B. Jones, R. Knight, F. Ogden, J. Selker, and O. Wendroth. 2008. Soil moisture measurement for ecological and hydrological watershed scale observatories: A review. Vadose Zone J. 7:358–389.

Robinson, D.A., C.M.K. Gardner, J. Evans, J.D. Cooper, M.G. Hodnett, and J.P. Bell. 2005. A physically derived water content/permittivity calibration model for coarse-textured, layered soils. Soil Sci. Soc. Am. J. 69:1372–1378.

Rodriguez-Iturbe, I., G.K. Vogel, R. Rigon, D. Entekhabi, F. Castelli, and A. Rinaldo. 1995. On the spatial organization of soil moisture fields. Geophys. Res. Lett. 22:2757–2760.

Rosenbaum, U., J.A. Huisman, A. Weuthen, H. Vereecken, and H.R. Bogena. 2010. Sensor-to-sensor variability of the ECH$_2$O EC-5, TE, and 5TE sensors in dielectric liquids. Vadose Zone J. 9:181–186.

Roth, K., R. Schulin, H. Flühler, and W. Attinger. 1990. Calibration of time domain reflectometry for water content measurement using a composite dielectric approach. Water Resour. Res. 26:2267–2273.

Ryu, D., and J.S. Famiglietti. 2005. Characterization of footprint-scale surface soil moisture variability using Gaussian and beta distribution functions during the Southern Great Plains 1997 (SGP97) hydrology experiment. Water Resour. Res. 41:W12433, doi:10.1029/2004WR003835.

Ryu, D., and J.S. Famiglietti. 2006. Multi-scale spatial correlation and scaling behavior of surface soil moisture. Geophys. Res. Lett. 33:L08404, doi:10.1029/2006GL025831.

Sakaki, T., A. Limsuwat, K.M. Smits, and T.H. Illangasekare. 2008. Empirical two-point α-mixing model for calibrating ECH$_2$O EC-5 soil moisture sensors in sand. Water Resour. Res. 44:W00D08, doi:10.1029/2008WR006870.

Schmidt, F. 2002. Topocrop terrain indices ArcView extension. Available at arcscripts.esri.com/details.asp?dbid = 12527 (verified 31 May 2010). ESRI, Redlands, CA.

Schulz, K., R. Seppelt, E. Zehe, H.J. Vogel, and S. Attinger. 2006. Importance of spatial structures in advancing hydrological sciences. Water Resour. Res. 42:W03S03, doi:10.1029/2005WR004301.

Seyfried, M. 1998. Spatial variability constraints to modelling soil water at different scales. Geoderma 85:231–254.

Snepvangers, J.J.J.C., G.B.M. Heuvelink, and J.A. Huisman. 2003. Soil water content interpolation using spatio-temporal kriging with external drift. Geoderma 112:253–271.

TERENO. 2010. Welcome to TERENO terrestrial environmental observatories. Available at www.tereno.net (verified 31 May 2010. Helmholtz Assoc., Berlin.

Thierfelder, T.K., R.B. Grayson, D. von Rosena, and A.W. Western. 2003. Inferring the location of catchment characteristic soil moisture monitoring sites: Covariance structures in the temporal domain. J. Hydrol. 280:13–32.

Topp, G.C., J.L. Davis, and A.P. Annan. 1980. Electromagnetic determination of soil water content: Measurements in coaxial transmission lines. Water Resour. Res. 16:574–582.

Transregional Centre 32. 2009. Patterns in soil–vegetation–atmosphere systems: Monitoring, modelling and data assimilation. Available at www.tr32.de (verified 31 May 2010). Transregional Collaborative Res. Ctr. 32, Meteorol. Inst., Univ. of Bonn, Bonn, Germany.

Trubilowicz, J., K. Cai, and M. Weiler. 2009. Viability of motes for hydrological measurement. Water Resour. Res. 45:W00D22, doi:10.1029/2008WR007046.

Valente, A., R. Morais, A. Tuli, J.W. Hopmans, and G.J. Kluitenberg. 2006. Multi-functional probe for small-scale simultaneous measurements of soil thermal properties, water content, and electrical conductivity. Sens. Actuators A: Phys. 132:70–77.

Vereecken, H., J.A. Huisman, H.R. Bogena, J. Vanderborght, J.A. Vrugt, and J.W. Hopmans. 2008. On the value of soil moisture measurements in vadose zone hydrology: A review. Water Resour. Res. 44:W00D06, doi:10.1029/2008WR006829.

Vereecken, H., T. Kamai, T. Harter, R. Kasteel, J. Hopmans, and J. Vanderborght. 2007. Explaining soil moisture variability as a function of mean soil moisture: A stochastic unsaturated flow perspective. Geophys. Res. Lett. 34:L22402, doi:10.1029/2007GL031813.

Walker, J.P., P.R. Houser, and G.R. Willgoose. 2004. Active microwave remote sensing for soil moisture measurement: A field evaluation using ERS-2. Hydrol. Processes 1811:1975–1997.

Western, A.W., and G. Blöschl. 1999. On the spatial scaling of soil moisture. J. Hydrol. 217:203–224.

Western, A.W., R.B. Grayson, and T. Green. 1999. The Tarrawarra project: High resolution spatial measurement, modelling and analysis of soil moisture and hydrological response. Hydrol. Processes 13:633–652.

Western, A.W., S.-L. Zhou, R.B. Grayson, T.A. McMahon, G. Blöschl, and D.J. Wilson. 2004. Spatial correlation of soil moisture in small catchments and its relationship to dominant spatial hydrological processes. J. Hydrol. 286:113–134.

Wigneron, J.-P., J.-C. Calvet, T. Pellarin, A.A. Van de Griend, M. Berger, and P. Ferrazzoli. 2003. Retrieving near-surface soil moisture from microwave radiometric observations: Current status and future plans. Remote Sens. Environ. 854:489–506.

Zehe, E., R. Becker, A. Bárdossy, and E. Plate. 2005. Uncertainty of simulated catchment scale runoff response in the presence of threshold processes: Role of initial soil moisture and precipitation. J. Hydrol. 315:183–202.

ZigBee Alliance. 2010. Zigbee Alliance. Available at www.zigbee.org/ (verified 31 May 2010). Zigbee Alliance, San Ramon, CA.